JTTEE5 19:384–391
DOI: 10.1007/s11666-009-9388-0
1059-9630/$19.00 © ASM International

Wear Behavior of Plasma-Sprayed Al-Si/TiB_2/h-BN Composite Coatings

I. Ozdemir, C. Tekmen, Y. Tsunekawa, and T. Grund

(Submitted April 24, 2009; in revised form July 27, 2009)

In this study, mechanically alloyed Al-12Si/TiB_2/h-BN composite powder was deposited onto aluminum substrates by atmospheric plasma spraying. Wear performance of the coating was investigated with respect to the structural evolution of the composite powder coating. Non-lubricated ball-on-disk tests were used to examine the wear resistance of the coatings. The worn surfaces were examined using scanning electron microscopy and energy dispersive spectroscopy to elucidate the wear mechanisms operating at the sliding interface. It has been observed that TiB_2 and in situ formed AlN and Al_2O_3 phases in combination with h-BN solid lubricant strongly affect the wear performance of the coating.

Keywords aluminum composites, APS coatings, friction and wear, influence of spray parameters

1. Introduction

Al-Si alloys are attractive in the production of internal combustion engine components due to their low density, favorable thermal properties, excellent corrosion resistance, and process flexibility. However, the major drawbacks of these alloys are a low hardness and a low wear resistance under loaded sliding conditions. Compared to other modification technologies, thermal spray processes have already found a wide application area in different industries by deposition of metallic, ceramic, or composite materials (Ref 1-4). Thermal spraying is an extremely fast deposition process for surface coatings with a thickness of over 100 μm. The deposition rate is approximately 1-10 mm/s or even more, which is at least 10 times higher than those of other conventional vapor phase deposition methods and conventional electroplating. Ceramic particles of SiC, TiB_2, B_4C, TiC, or Al_2O_3 can be used to reinforce thermally sprayed Al-based coatings to improve their anti-wear performance. Among these materials, titanium diboride (TiB_2) is an advanced ceramic material with relatively high strength and durability provided by a high-melting point, high hardness, excellent strength-to-density ratio, and high wear resistance (Ref 5-8). In addition to hard ceramic reinforcements, hexagonal boron nitride (h-BN) is a promising incorporation in aluminum metal matrix composites due to its low density, excellent stability, high thermal conductivity, and good lubricity (Ref 9-12). Plasma-sprayed coatings containing h-BN as a solid lubricant which was incorporated into the starting materials by spray-drying method exhibits a better tribological behavior (Ref 13). It has been shown that thermally sprayed coatings containing solid lubricants like graphite, Teflon (PTFE), MoS_2, MnS, or CaF_2 reduce the energy loss by friction and weight loss by wear (Ref 14). Moreover, the size and uniform distributions of the solid lubricant as well as the wetting condition, adhesion, and interaction of the solid lubricant with the feedstock material affect strongly the tribological properties of the coating (Ref 14-16). However, during reactive plasma spraying in situ formed phases are thermodynamically more stable and promise a better cohesion which lead to improved coating properties (Ref 5).

In this study, mechanically alloyed Al-12Si/TiB_2/h-BN composite powder was deposited onto aluminum substrates by atmospheric plasma spraying (APS). Wear performance of the coatings has been investigated.

2. Experimental Studies

Al-12Si (Metco 52C-NS, Sulzer Metco (Japan) Ltd., Tokyo, Japan) powder manufactured by a gas atomization process with a particle size range of −106 +32 μm, high purity (>99%) TiB_2 powder (16 wt.%) with an average

This article is an invited paper selected from presentations at the 2009 International Thermal Spray Conference and has been expanded from the original presentation. It is simultaneously published in *Expanding Thermal Spray Performance to New Markets and Applications: Proceedings of the 2009 International Thermal Spray Conference*, Las Vegas, Nevada, USA, May 4-7, 2009, Basil R. Marple, Margaret M. Hyland, Yuk-Chiu Lau, Chang-Jiu Li, Rogerio S. Lima, and Ghislain Montavon, Ed., ASM International, Materials Park, OH, 2009.

I. Ozdemir, Department of Metallurgical & Materials Engineering, Bartın University, 74100 Bartın, Turkey; **C. Tekmen** and **Y. Tsunekawa**, Materials Processing Laboratory, Toyota Technological Institute, 2-12-1 Hisakata Tempaku, 468-8511 Nagoya, Japan; and **T. Grund**, Fakultät für Maschinenbau, Technische Universität Chemnitz, Lehrstuhl für Verbundwerkstoffe, Erfenschlager Str. 73, 09125 Chemnitz, Germany. Contact e-mail: ismail.ozdemir@deu.edu.tr.

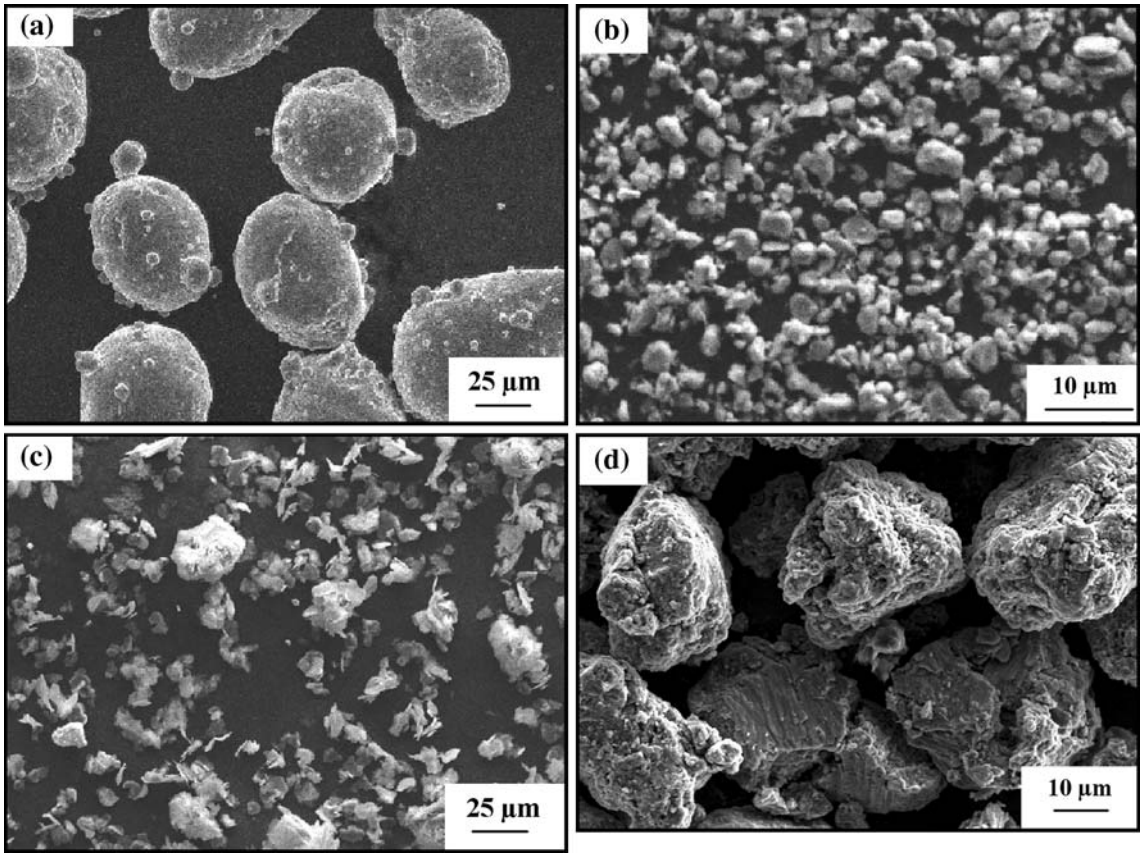

Fig. 1 SEM micrographs showing the morphology of (a) Al-12Si, (b) TiB_2, (c) h-BN, and (d) 5 h MA powder

particle size of 73 μm and a h-BN powder (7.7 wt.%) with an average particle size of 16 μm were used as starting materials. Powders were mechanically alloyed (MA) at 100 rpm for 1, 3, 5, 7, 15, 24, and 48 h. After the MA process, the composite powders were sieved to a particle size fraction of −100 +32 μm. The morphology of the starting powders and after 5 h MA is shown in Fig. 1. More details regarding the preparation of the composite powder, the MA process and powder properties can be found in a previous study (Ref 17).

Blasted $30 \times 30 \times 5$ mm^3 pure aluminum (A1050) plates were prepared as substrates. To prevent any partial melting during plasma spraying, the substrate temperatures were continuously recorded by thermocouples that were inserted centered. The substrates were continuously cooled from the backside via an air cooling nozzle. Coating experiments were carried out using an APS set (Sulzer Metco 9 M, Tokyo, Japan) under conditions given in Table 1. Wear tests were carried out by means of a ball-on-disk tribo-test (Tetra GmbH, Ilmenau, Germany) in sliding condition without lubricant and in air (ASTM D 6425). Hardened 100Cr6 stainless steel and Al_2O_3 balls (diameter, 6 mm) were used as counterparts. Wear tests were performed by applying 5 N load with a rotation speed of 80 rpm and a total wear distance of 0.5 km. As reference, tests were also performed on pure aluminum substrates. At least, three repetitions of each test were carried out. Surfaces of the coatings and substrate were metallographically prepared to a surface finish of 1.6 μm (R_a) prior to wear tests. Surface roughnesses as well as depths of wear tracks were measured by stylus profilometry (Mitutoyo, SJ-301, Kawasaki-shi, Kanagawa, Japan). The volumetric wear loss was determined by means of optical 3D profilometry and software-aided analysis of wear tracks (MicroCAD compact stripe profilometer, GF Messtechnik GmbH, Berlin, Germany). The morphology of wear scars and tribological deposits were examined by scanning electron microscopy (SEM, LEO 1455VP, Carl Zeiss AG, Oberkochen, Germany). Microhardness measurements were carried out using a Vickers hardness tester and 200 g load (Shimadzu HSV-30, Kyoto, Japan).

Table 1 Spray parameters for spraying Al-Si/TiB_2/h-BN powders

Parameter	Value
Arc current	400 (A)
Primary gas, Ar	40 (L/min)
Secondary gas, H_2	6 (L/min)
Carrier gas, Ar	4 (L/min)
Spray distance	100 (mm)
Powder feeding rate	8 (g/min)

3. Results and Discussion

The effect of the MA time on the powder morphology, size, composition, and reaction intensity between selective powders has been investigated in previous studies in which it has been observed that with increasing the MA time, the resulting powder morphology changes from flaky to spherical (Ref 17). Furthermore, the decomposition rate of h-BN and the in situ reaction intensity between the selective powders during plasma spraying also increase (Ref 17). Considering the APS-parameters, it has been demonstrated that increasing the arc current leads to precipitation and growth of Si particles, which consequently causes a decrease in the coating hardness. In contrast, increasing the secondary gas (H_2) flow rate is only effective at relatively high arc currents and induces a reaction between the different powder phases resulting in an increased hardness. In this study, coatings were prepared with an optimum MA (Ref 17) and spray parameters (Table 1) to obtain a relatively high h-BN content in the coatings in order to achieve a good wear performance.

3.1 Microstructure

A typical cross section microstructure of the coating is shown in Fig. 2(a), where the coating exhibits a lamellar structure, a low amount of both un-melted particles and pores and an average thickness of ~250 μm. Black zones observed in the microstructure result from pores and inclusions as well as semi-melted particles. The formation of micropores during the solidification is inevitable, especially, when spraying in air. This phenomenon is linked to gas entrapment during splats pile-up. Dark-brown regions observed in the microstructure (Fig. 2b) are formed by the h-BN solid lubricant. Also, the observation of oxide layers in the coating microstructures indicates that aluminum is slightly oxidized during the MA or coating process (in-flight or after impinging the substrate) (Fig. 2b). SEM observations clearly show that TiB_2 is well-dispersed throughout the matrix (Fig. 2c). Elemental distribution of Al, Si, O, and Ti in coating cross sections was determined by EDS (Fig. 3). Since elemental distributions of boron and nitrogen cannot be distinguished due to the relatively low atomic weight, regions with relatively high intensities of oxygen and titanium correspond to Al_2O_3 and TiB_2, respectively. However, as seen from the back-scattered electron (BSE) image, some dark-gray regions and spherical structures were observed. Quantitative point analyses performed within these regions (Fig. 4a, b) demonstrate that those round light-gray structures consist mainly from Al and very low Si and might correspond to semi- or un-melted Al-Si particles that remained from the MA process. In contrast, the dark-gray regions contain more Si which may be linked to the solidification rate of the individual splat. Also, some dark-gray round type structures in size of 500 nm were observed (Fig. 4b) consisting mainly from Al. These structures may correspond to in situ formed AlN owing significant concentration (25%) in the coatings.

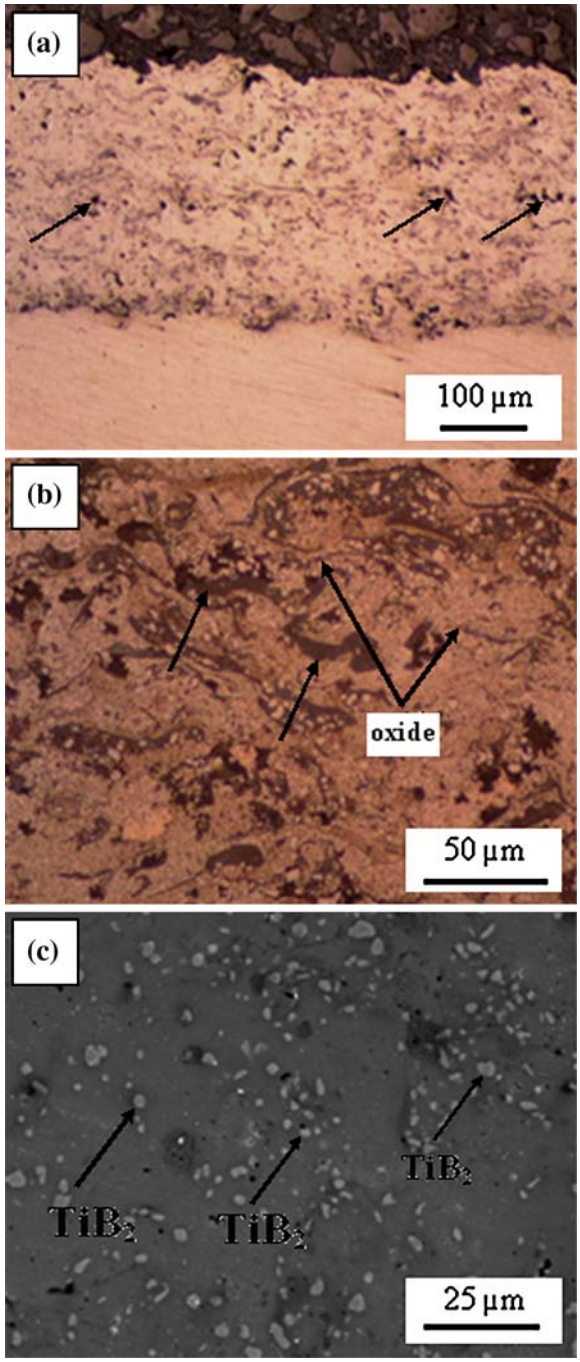

Fig. 2 Typical cross section microstructure of the coating (a, b) optic and (c) SEM

3.2 Friction and Wear Characteristics

In order to examine the capability for load bearing, Al-based composite coatings were subjected to wear by using a ball on disc configuration under dry condition in air. Wear tests were performed against 100Cr6 and Al_2O_3 balls. Depending on the particular material combination, test duration and test load, the prevailing mechanism of adhesive, abrasive, and fatigue wear show different

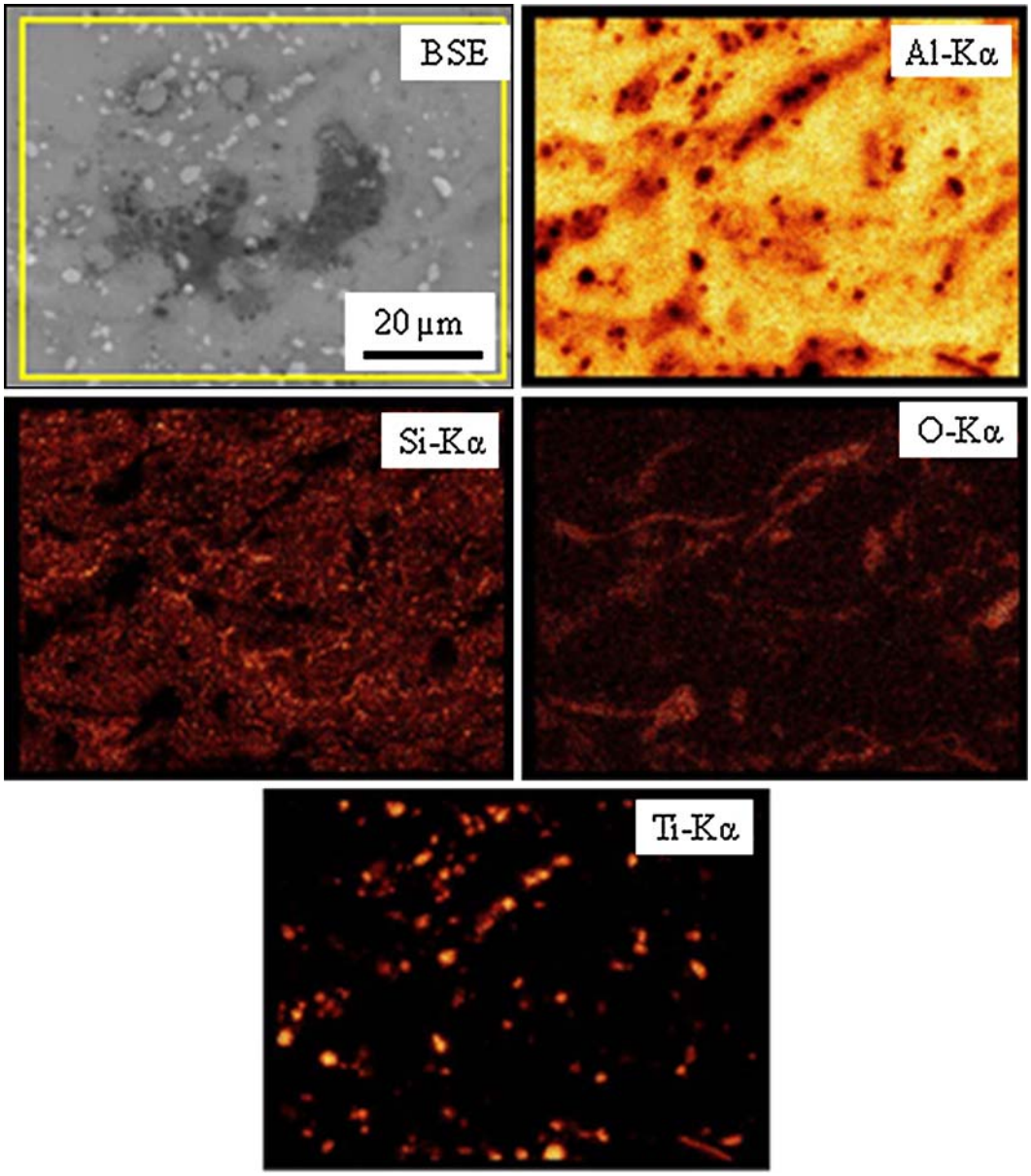

Fig. 3 Back-scattered image and elemental mapping of Al, Si, O, and Ti

intensities. The behavior of the friction coefficient during the tests is presented in Fig. 5. The friction coefficient evolves through two stages which are linked to the running-in and the stable state of the tribological system. Figure 5 also depicts that the friction coefficient decreases with an increase in load. The friction coefficient of the composite coating is higher than that of substrate tested at 5 N. However, increasing the normal load from 5 to 10 N, the friction coefficient of the coating becomes smaller than the substrate. The reduction in friction coefficient of the coating at the highest load, 10 N, can be attributed to the smoothness of the surface which takes place as a result of sliding against the hard surface of the counter material and a possible densification of the coating's top-layer. Such observation was clarified by Mandal et al. (Ref 18) that at higher loads, the formation of a stable mechanically mixed layer leads to decrease in the frictional force. Moreover, it was expected that the presence of the h-BN solid lubricant would reduce the friction coefficient of plasma-sprayed composite coating. However, the content and uniformity of the solid lubricant inside the matrix structure strongly affects the tribological performance. An insufficient amount of solid lubricant may result in an increase in friction and wear loss. On the other hand, an excessive level of solid lubricant undermines wear performance and mechanical properties as well. In addition to this, the study carried out by Zorawski et al. (Ref 19) showed that the optimization of the plasma spray parameters is required to obtain a composite coating containing solid lubricant, CaF_2 (22 vol.%), with a smaller

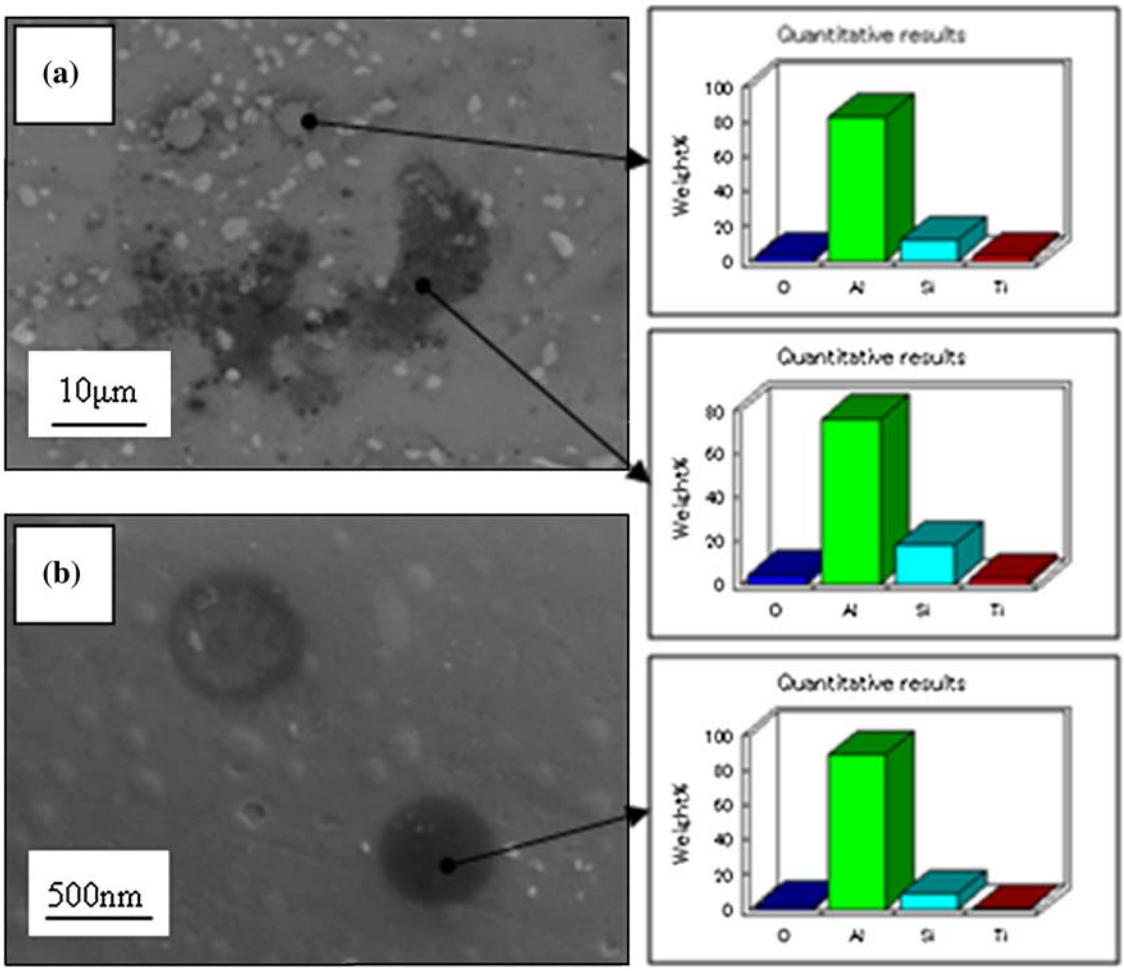

Fig. 4 SEM images and EDS point analyses of different structures

friction coefficient. The maximum friction coefficient is about 0.8 for the coatings, whether the counter-bodies were 100Cr6 or Al_2O_3 balls (Fig. 5b). On the other hand, the friction value (average value 0.85) of pure Al-substrate was found to be slightly higher than the coatings tested with similar conditions. When increasing the wear test load to 10 N, a transition from a mild-to-severe wear was observed, therefore wear test load of 5 N was fixed for all tests. Although the friction coefficients of both the tribological systems tested (100Cr6 and Al_2O_3 ball) did not vary much (Fig. 5b), the volumetric wear loss of coatings tested against 100Cr6 ball is much lower than for those tested with an Al_2O_3 ball (Fig. 6). The results presented in the Fig. 6 represent the average of three independent experiments. This may be attributed to differences in the wear mechanism since the 100Cr6 ball slightly worn out during the test, due to abrasive wear on it. Besides, it has been observed that the 100Cr6 ball surface was cladded with the coating materials. So, the adhesive wear mechanism and thus, the mere deforming of the surface material seems to be higher in this configuration than in tribological systems with Al_2O_3 as the counter material. Even though the coating hardness is much lower than the counter-body, the observation of wear tracks on the stainless steel balls may result from the abrasive effect of the hard phases such as TiB_2 distributed well inside the coating. The hardness levels of the coatings are related to several factors including the feedstock characteristics, degree of the molten particles, splat/substrate interface formation, and spray plasma properties. Especially in the case of using eutectic Al-Si-alloy, in-flight particle and substrate conditions strongly affect the solidification rate and thus the forming and growth of Si-precipitations in the Al-matrix and cause a decrease in the matrix hardness due to a lowered solid-solution hardening. However, in previous studies (Ref 5, 17), it has been shown that the hardness profiles of the coatings strongly depend on the amount of TiB_2 and in situ formed AlN and Al_2O_3 during the APS process. SEM observations of Vickers hardness indentations (Fig. 7) clearly demonstrate the crack propagation through the matrix. The depths of wear tracks are well consistent with the volumetric wear loss measurements. Typical surface profiles of the substrate and coatings wear tested against both types of balls are presented in Fig. 8. Characteristic topography of the worn coating tested against an Al_2O_3 ball at a load of 5 N is shown in

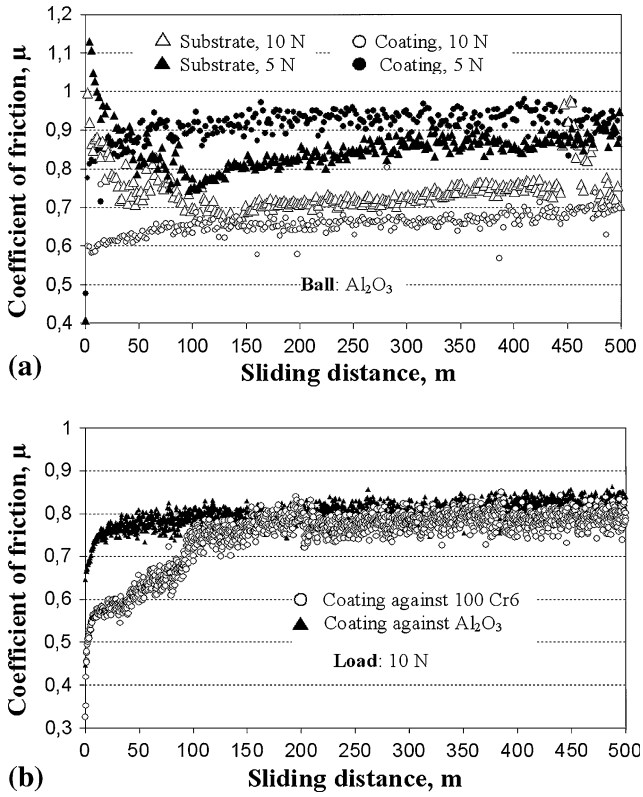

Fig. 5 Change in friction coefficient of materials tested (a) at 5 and 10 N (b) against different balls

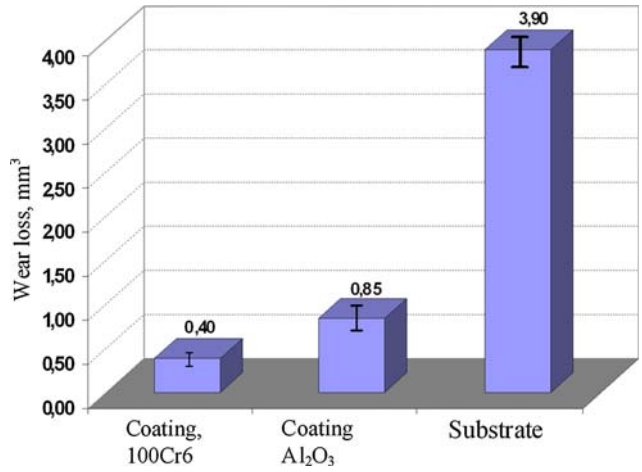

Fig. 6 Comparison of the volume loss for tested materials after the dry ball on disc wear test at 5 N

Fig. 8(d), which shows a smoothening of the surface due to wear. The significant reduction of the wear depths of the coatings can be attributed to the higher surface hardness which avoids the transition to severe wear as it was observed on the aluminum substrate. Examination of the worn coating surfaces revealed a different appearance compared to the substrate (Fig. 9). The Al-substrate showed a strong plastic deformation and extrusion at the

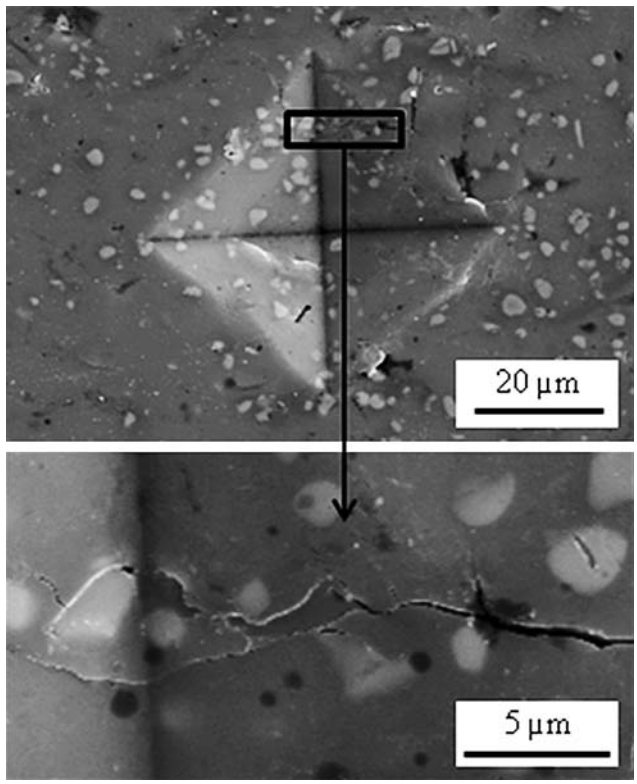

Fig. 7 SEM image of the Vickers hardness indentation

edges of the wear track. The thermally sprayed coatings were also plastically deformed, but did not show deformation lips at the edges of wear tracks (Fig. 9b). The top-layers of the coatings were only slightly flattened toward the sliding direction. At higher magnification, surface cracking or removal of coating forming particles was detected. The content of fine-dispersed hard-phases (Fig. 9c) and the combination with solid lubricant lower the intensity of adhesive and abrasive wear mechanism and further decrease the wear loss in comparison to the pure Al-substrate. The role of hard particles such as Al_2O_3, TiB_2, AlN in the coating help reduce intrinsically the material removal by resisting further plastic deformation compared to the soft aluminum substrate. On the other hand, these hard particles may develop higher amount of contact stress during the ball on disc test which might possibly lead to a heightened share of fatigue wear resulting in cracking, splat delamination, and thus in an accelerate wear rate.

4. Conclusions

This study has investigated the wear performance of plasma-sprayed Al-12Si/TiB_2/h-BN composite coatings. The major results are summarized as follows:

– The particle microstructures and properties of the Al-based MA composite spray powder are successfully transferred into the APS coatings.

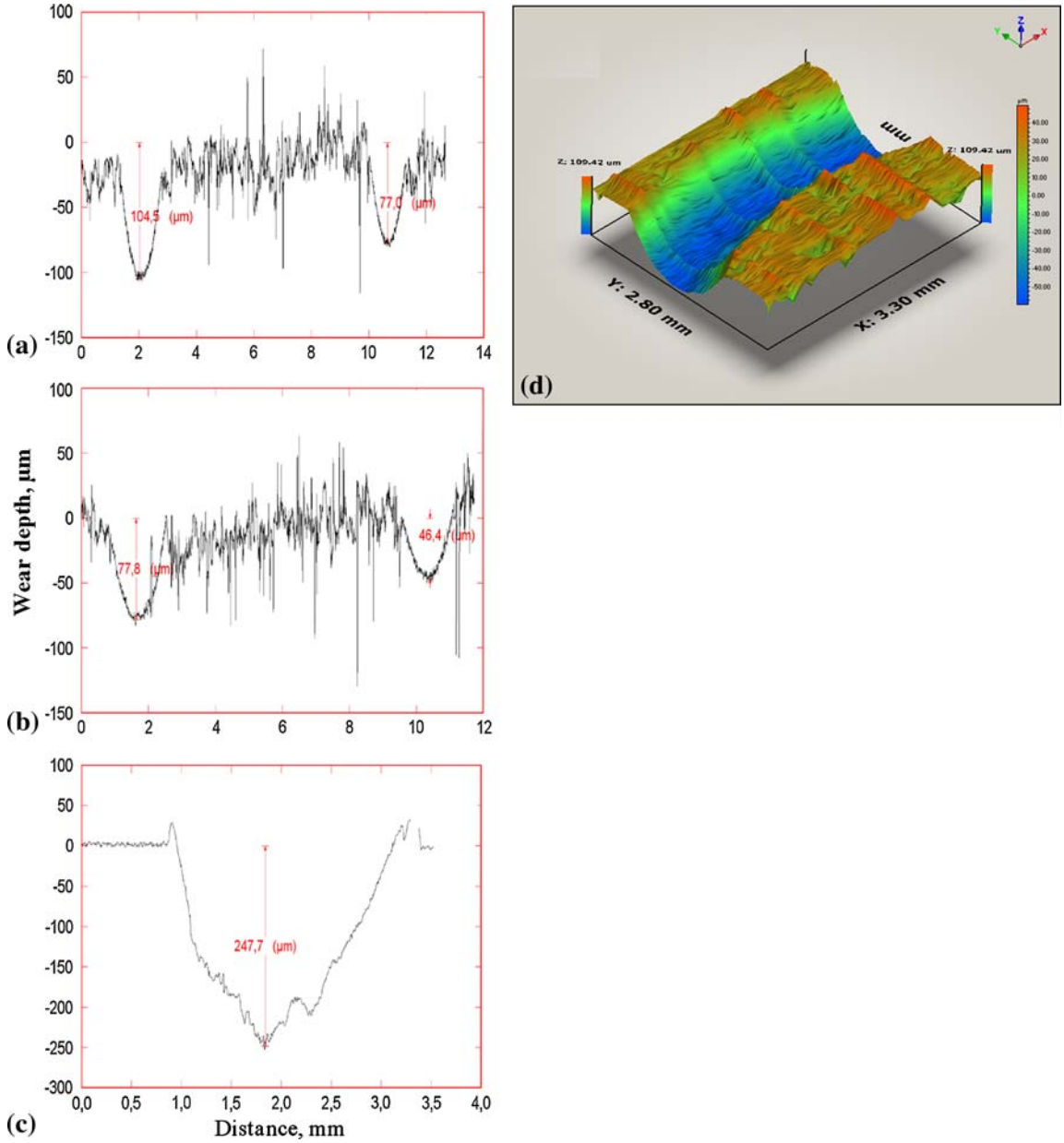

Fig. 8 Surface profile of coatings wear tested against (a) Al_2O_3, (b) 100 Cr6, (c) substrate, and (d) surface topography of the worn coating

- EDS investigations revealed the probable in situ formation of reactive hard-phases, such as AlN and Al_2O_3.
- The presence of solid lubricant, h-BN (7.7 wt.%), had no significant influence in reducing the friction coefficient of the plasma-sprayed coatings as compared to the that of the substrate. The maximum friction coefficient was found to be approximately 0.8 for the coatings, whether the counter-bodies were 100Cr6 or Al_2O_3 balls.
- The role of counter material plays an important role in reducing the volume loss of the coatings after wear test. The volume loss of the coating was measured approximately two times higher when it was wear tested against Al_2O_3 ball instead of 100Cr6 ball.
- In addition to h-BN, the presence of these hard-phases (Al_2O_3, AlN) and added TiB_2 within the APS-sprayed Al-based coatings significantly improve the superficial wear resistance in comparison to pure Al-substrate. The dominant wear mechanism of the plasma-sprayed coatings was surface cracking and removal of coating by splat delamination. Plowing and strong plastic deformation together with extrusion at the edges of wear track controlled the wear process in Al-substrate.

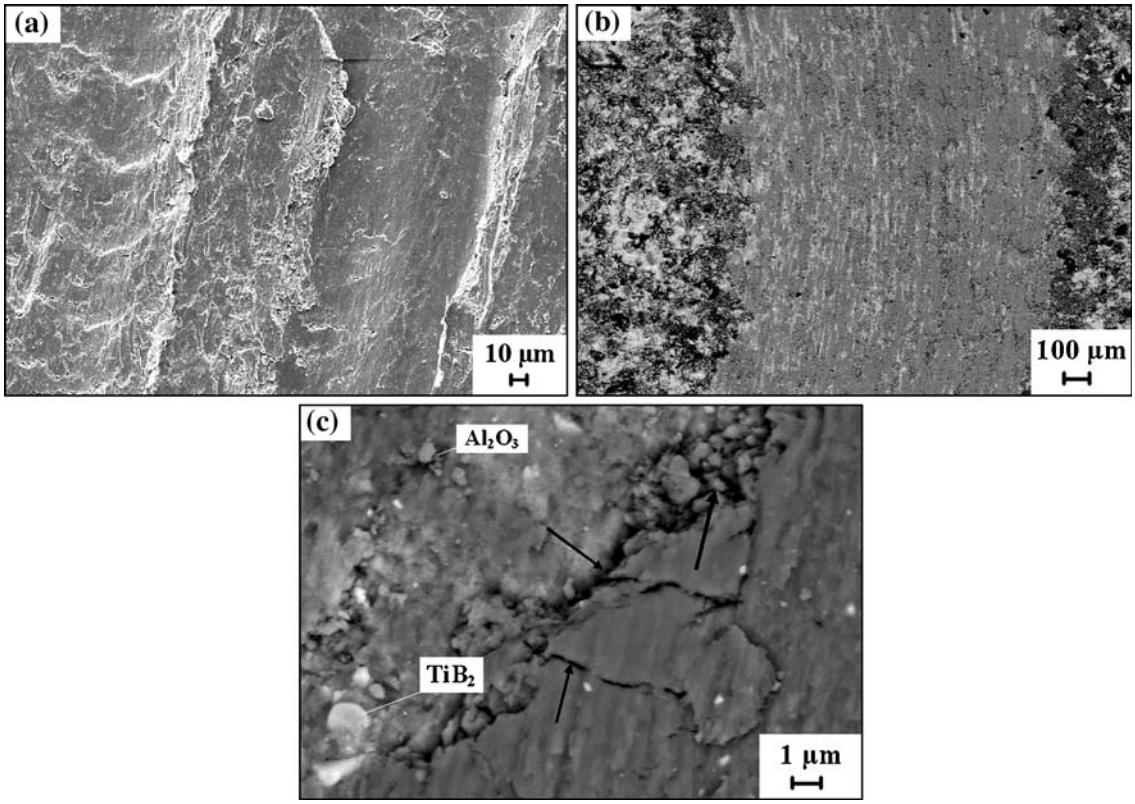

Fig. 9 SEM micrographs showing the morphologies of the worn surfaces of (a) pure Al-substrate, (b) and (c) sprayed coatings tested at 5 N and 80 rpm rotational speed

References

1. G. Barbezat, Application of Thermal Spraying in the Automobile Industry, *Surf. Coat. Technol.*, 2006, **201**, p 2028-2031
2. G. Pirge, Characterization of Thermal Barrier Coated Various Aerospace Alloys, *Aircraft Eng. Aerospace Technol.*, 2008, **80**(4), p 359-364
3. A. Sanz, New Coatings for Continuous Casting Rolls, *Surf. Coat. Technol.*, 2004, **177-178**, p 1-11
4. M. Gaona, R.S. Lima, and B.R. Marple, Nanostructured Titania/Hydroxyapatite Composite Coatings Deposited by High Velocity Oxy-Fuel (HVOF) Spraying, *Mater. Sci. Eng.*, 2007, **458**(1-2), p 141-149
5. C. Tekmen, Y. Tsunekawa, and M. Okumiya, In Situ TiB_2 and Al_2O_3 Formation by DC Plasma Spraying, *Surf. Coat. Technol.*, 2008, **202**(17), p 4170-4175
6. A. Calka and D. Oleszak, Synthesis of TiB_2 by Electric Discharge Assisted Mechanical Milling, *J. Alloys Compd.*, 2007, **440**(1-2), p 346-440
7. A. Mandal, M. Chakraborty, and B.S. Murty, Effect of TiB_2 Particles on Sliding Wear Behavior of Al-4Cu Alloy, *Wear*, 2007, **262**, p 160-166
8. R. Ricceri and P. Matteazzi, A Fast and Low-Cost Room Temperature Process for TiB_2 Formation by Mechanosynthesis, *Mater. Sci. Eng.*, 2004, **379**(1-2), p 341-346
9. Z.P. Xia, Z.Q. Li, C.J. Lu, B. Zhang, and Y. Zhou, Structural Evolution of Al/BN Mixture During Mechanical Alloying, *J. Alloys Compd.*, 2005, **399**(1-2), p 139-143
10. Y. Li, J. Zhang, G. Qiao, and Z. Jin, Fabrication and Properties of Machinable 3Y-ZrO_2/BN Nanocomposites, *Mater. Sci. Eng.*, 2005, **397**(1-2), p 35-40
11. X. Wang, G. Qiao, and Z. Jin, Preparation of SiC/BN Nanocomposites Powders by Chemical Processing, *Mater. Lett.*, 2004, **58**, p 1419-1423
12. A. Anal, T.K. Bandyopadhyay, and K. Das, Synthesis and Characterization of TiB_2-Reinforced Iron-Based Composites, *J. Mater. Proc.*, 2006, **172**(1), p 70-76
13. Y. Tsunekawa, I. Ozdemir, and M. Okumiya, Plasma Sprayed Cast Iron Coatings Containing Solid Lubricant Graphite and h-BN Structure, *J. Therm. Spray*, 2006, **15**(2), p 239-245
14. U. Mannikko, A. Maatta, P. Vuoristo, and T. Mantyla, Preparation and Characterization of Powders and Coatings Containing Solid Lubricants, *Thermal Spray 2003: Advancing the Science and Applying the Technology*, B.R. Marple and C. Moreau, Ed., May 5-8, 2003 (Orlando, FL), ASM International, 2003, Vol 1, 845 p; Vol 2, 864 p
15. I. Ozdemir, Wear/Friction Behaviour of FeB and FeB/h-BN Coatings Sprayed by Atmospheric Plasma Spraying, *Prakt. Metallogr-PR M*, 2007, **44**(8), p 355-371
16. C. Tekmen, M. Yamazaki, Y. Tsunekawa, and M. Okumiya, In Situ Plasma Spraying: Alumina Formation and In-Flight Particle Diagnostic, *Surf. Coat. Technol.*, 2008, **202**(17), p 4163-4169
17. C. Tekmen, I. Ozdemir, G. Fritsche, and Y. Tsunekawa, Structural Evolution of Mechanically Alloyed Al-12Si/TiB2/h-BN Composite Powder Coating by Atmospheric Plasma Spraying, *Surf. Coat. Technol.*, 2009, **203**, p 2046-2051
18. A. Mandal, B.S. Murthy, and M. Chakraborty, Wear Behaviour of Near Eutectic Al-Si Alloy Reinforced With In Situ TiB_2 Partciles, *Mater. Sci. Eng.*, 2009, **506**, p 27-33
19. W. Zorawski, R. Chatys, N. Radek, and J.B. Jamrozek, Plasma-Sprayed Composite Coating with Reduced Friction Coefficient, *Surf. Coat. Technol.*, 2008, **202**, p 4578-4582